Neuron, Volume *91*

Supplemental Information

Mechanism of High-Frequency Signaling at a Depressing Ribbon Synapse

Chad P. Grabner, Charles P. Ratliff, Adam C. Light, and Steven H. DeVries

Supplemental Data

Figure S1

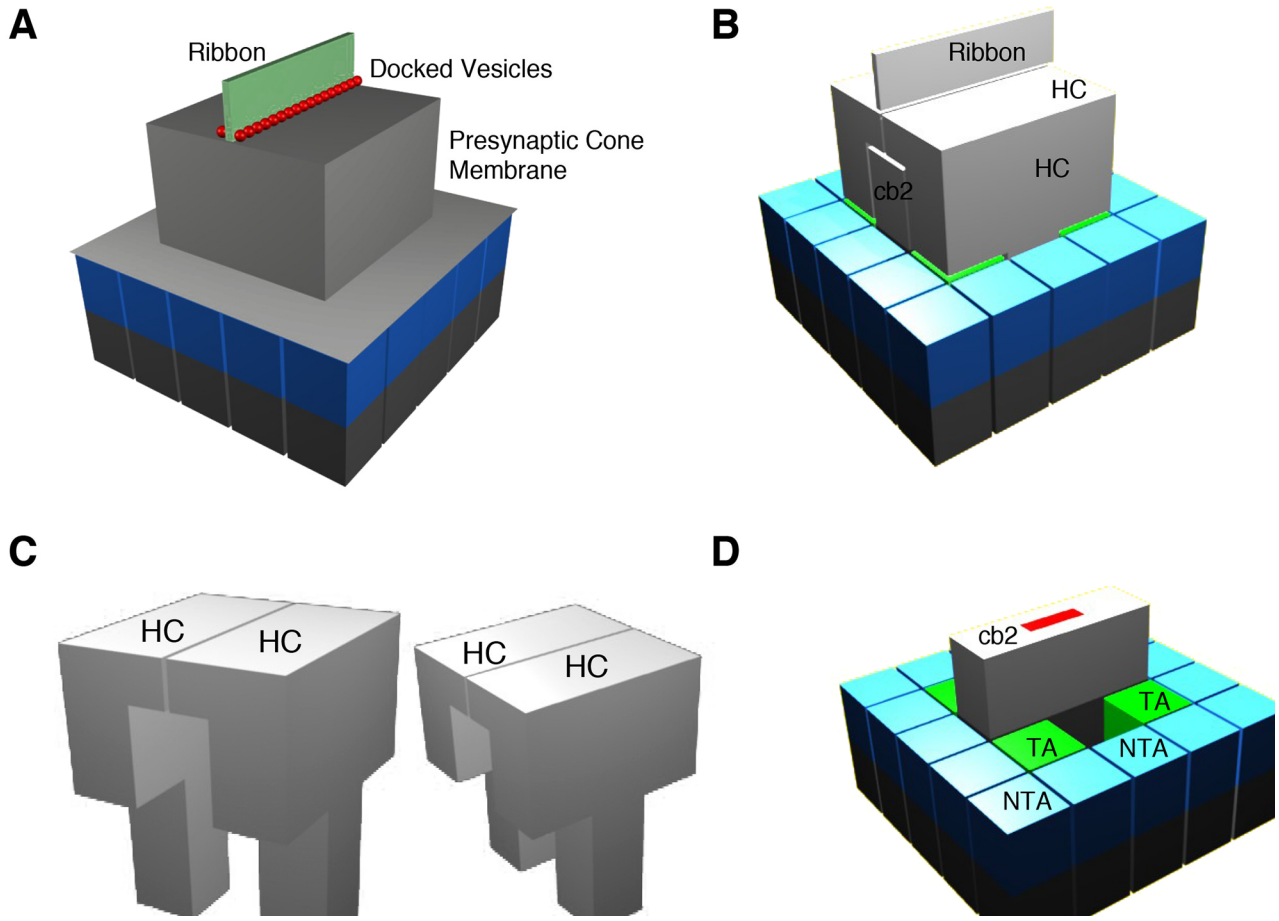

Figure S1, related to Figure 7: Model of the cone synapse. **A.** Ribbon (green) with docked vesicles (red) sits atop a single invagination of the presynaptic cone membrane (gray box). The basal synaptic surface is composed of bipolar cell dendritic contacts (dark gray and blue). In our simulations, the presynaptic membrane was first extended horizontally, then downward, and then horizontally again to cover the basal contacts as a sheet. **B.** Similar view to Figure 7A with the presynaptic cone terminal membrane and vesicles removed. The ribbon is maintained as a landmark. Glutamate released at the ribbon may diffuse both centrally and laterally between and around the horizontal cell (HC) processes to reach the basal postsynaptic surface. **C.** HC processes, shown from two different angles, occupy the bulk of the volume of the invagination. The AMPA receptors on HCs were not included in the model. **D.** Postsynaptic bipolar cells (right) with ribbon and HC processes removed. A single, invaginating bipolar cell contact (light grey) expressing AMPA receptors (red) was used instead of several separate invaginating contacts, some from On bipolar cells, so as to study differences in receptor placement. The basal region shows two types of bipolar cell processes. The green contacts below the removed HC processes (triad associated, TA) are closer to the invagination or triad than the blue bipolar cell contacts (non-TA, NTA), and were separately analyzed. For the present work, we note that neither type of basal process exhibited saturation.

Figure S2

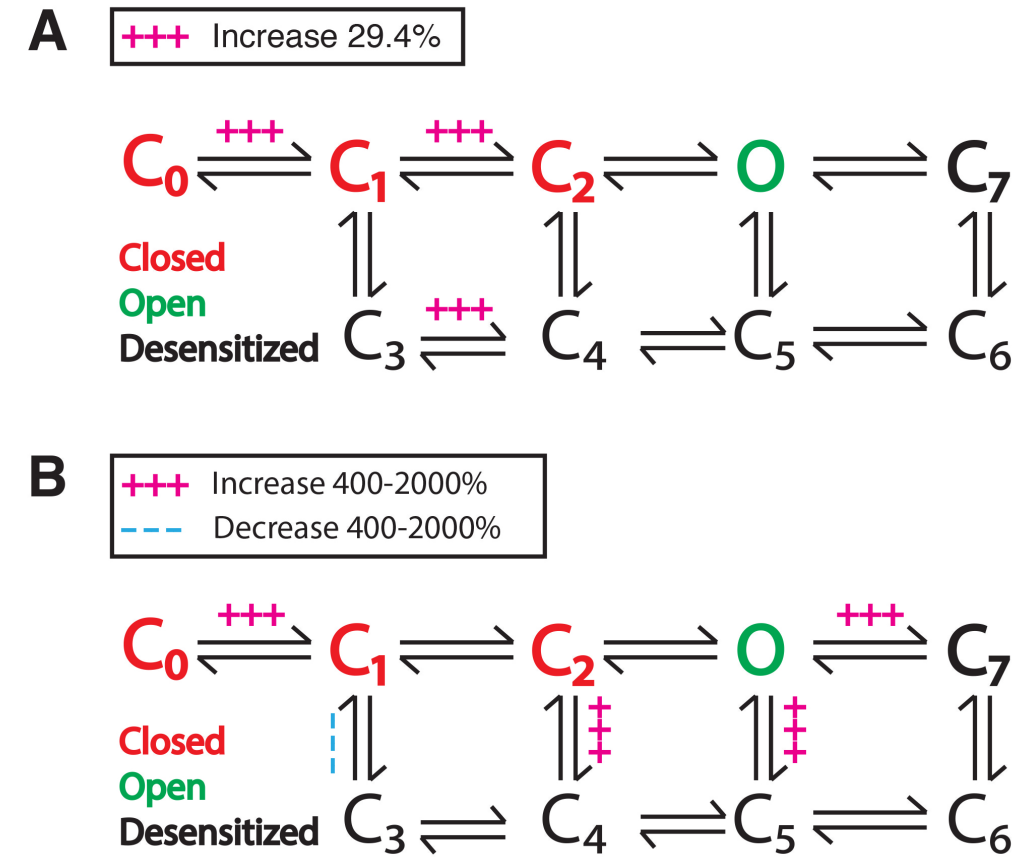

Figure S2, related to Figure 7: Since our goal was to address receptor saturation, which depends largely upon glutamate affinity and much less upon the decay phase of the EPSC, we initially modified the rate constants of the Häusser & Roth (1997) model to increase the affinity for glutamate from 440 to 340 μM. **A.** To increase affinity, the rate constants C_0-->C_1, C_1-->C_2 and C_3-->C_4 which involve glutamate binding were all increased by 29.4%. We increased the 'on' instead of decreasing the 'off' rates to better match the faster time course of the experimental mEPSC. Changing C_0-->C_1 alone, even by up to 1000-fold, had only a minor effect on response shape. **B.** Without further adjustment, the decay phase of the simulated mEPSC was still slower than the decay phase of the cb2 cell mEPSC (see Figure S3). The scheme was further modified to increase the rate of exit from the open state or the decay phase of the mEPSC, while preserving microscopic reversibility (DiGregorio et al., 2007).

Figure S3

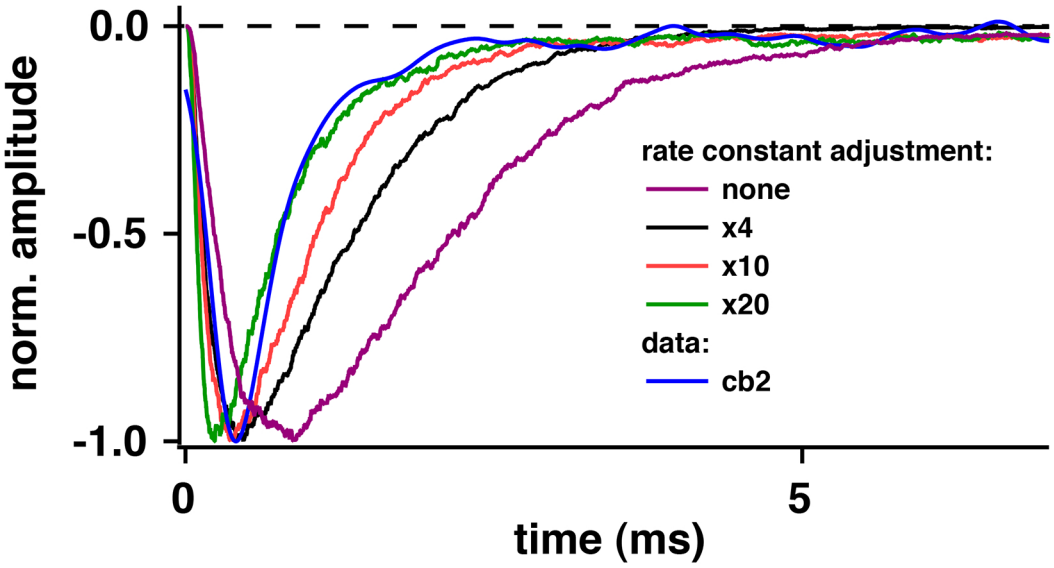

Figure S3, related to Figure 7: Speeding up the mEPSC time course. After making the affinity adjustment, we sought to match the response rise. A 10-fold increase in rate constant was selected as providing the best match between experimental and simulated events. The rate constants in Figure S2B were modified accordingly. The effects on saturation of making this second set of adjustments were minimal: EC_{50} was 3.4 versus 3.3 vesicles before and after the receptor modifications (data not shown; simulated with each vesicle containing 3000 glutamate molecules).

Figure S4

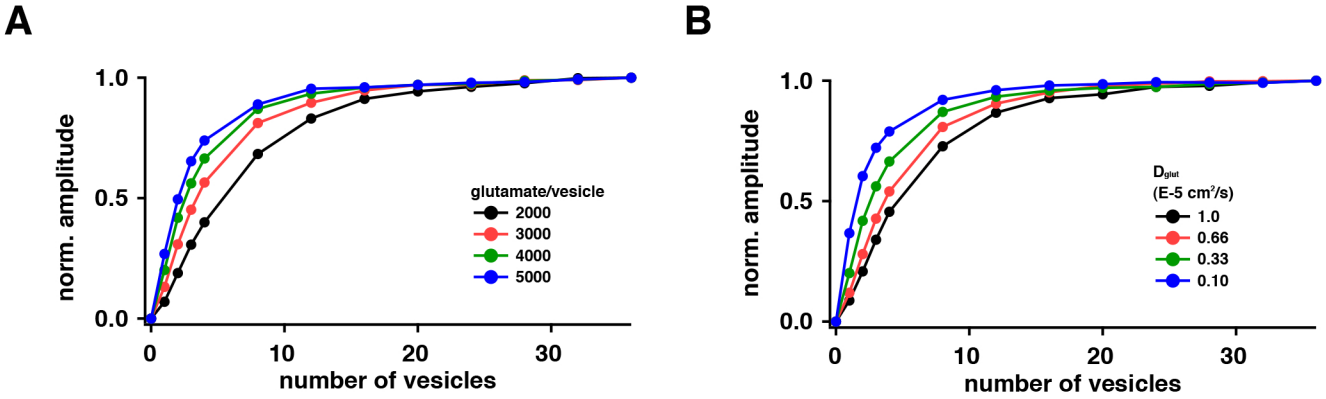

Figure S4, related to Figure 7: Control simulations of receptor saturation at the cone to cb2 cell synapse. **A.** Normalized EPSC amplitude versus number of vesicles released for different values of vesicular glutamate content. We varied the vesicular glutamate content from 2000 to 5000 per vesicle to ensure that receptor saturation was robust to the experimental uncertainty in estimating this quantity. **B.** Normalized EPSC amplitude versus number of vesicles released for different values of the glutamate diffusion constant.

Figure S5

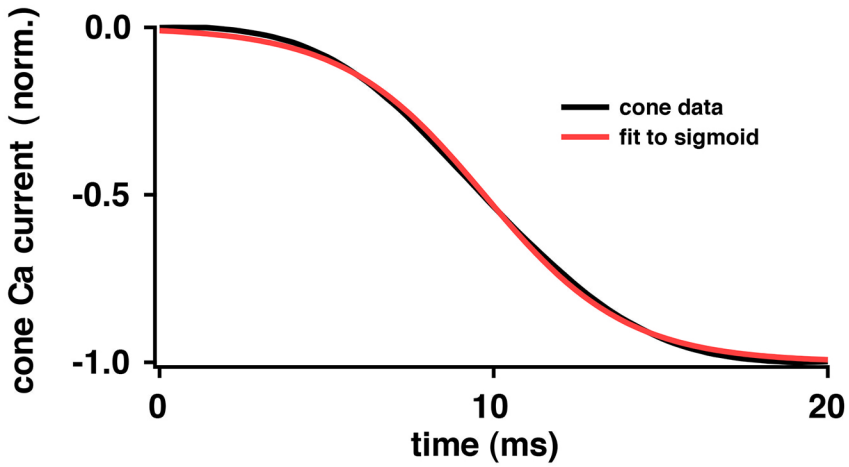

Figure S5, related to Figure 7: Time course of Ca^{2+} current activation at light-off with data fit to a sigmoid. The time course of the cone membrane voltage response at light-off was obtained from the traces in Figure 2 (*inset*). Membrane voltage was converted to Ca^{2+} current using the cone Ca^{2+} I-V relation (DeVries and Schwartz, 1999). The cone Ca^{2+} current versus time plot was fitted with a sigmoid. The sigmoid was taken as the cumulative probability distribution function for vesicle release times, and the vesicle release times used for each independent simulation were drawn randomly from this distribution.

Condition	Pulse duration (ms)	Recovery t (ms)	±SEM	n	p*
whole cell					
BAPTA, 10 mM	15	154.9	30	4	-
EGTA, 10 mM	1-15	133.5	23.3	8	-
loose seal	1	105.4	13.1	12	-
	5-15	125.1	22.8	6	-

*Wilconxon rank-sum test

Table S1, related to Figure 2: Recording conditions that can change the intracellular Ca^{2+} concentration or buffering do not affect paired pulse recovery. Paired pulse recovery at cone to cb2 cell synapses was statistically indistinguishable with respect to cone recording mode, whole cell or loose seal, duration of the cone step (1 – 15 ms), or intracellular Ca^{2+} buffer type, BAPTA or EGTA, both 10 mM. (-) indicates that none of the conditions produce statistically distinct results.

Condition	Control	CTZ (50-60 μM)	n	p*
Recovery tau (ms)	149.7±26.1	135.5±12.9	5	0.43
Peak amplitude (pA)	-311.3±64.4	-319.9±69.5	7	0.52

*Paired t test

Table S2, related to Figure 2: Effects of CTZ on paired-pulse recovery time course and EPSC amplitude. Recovery and control values were statistically indistinguishable.

Supplemental Experimental Procedures

Synapse model

The model synapse was based on published EM reconstructions of the cone terminal (Dowling and Boycott, 1966; Herr et al., 2011; Schein et al., 2011; Sterling and Matthews, 2005). The model featured a synaptic ribbon, a cone membrane that formed the presynaptic side of the cleft, two invaginating horizontal cell processes, and three types of bipolar cell processes: central (invaginating), triad-associated (TA, semi-invaginating), and non-triad-associated (NTA, basal). Vesicles were spaced 40 nm apart on both sides of the ribbon, invagination depth was 500 nm, bipolar cell contacts at the cone base were spaced 250 nm apart, and cleft width was 16 nm**.** Two horizontal cell processes abut at the base of the ribbon to form a sheet-like cleft through which glutamate can diffuse from ribbon to postsynaptic cb2 bipolar cell receptors. The receptors on the cb2 cells occupy a central patch that has 1/9 of the area of the entire surface (0.019 μm^2). Changing the size of this patch had only a small effect on the approach to saturation. We used the MCell default density for the AMPA receptors, 10,000-μm^{-2} (Stiles et al., 1996). For comparison, the maximal packing density of tetrameric GluA2-containing AMPA receptors is estimated to be 7400-μm^{-2} (Sobolevsky et al., 2009). We assumed that glutamate was instantaneously released upon vesicle fusion in line with empirical results from amperometric measurements at ribbon synapses (Grabner and Zenisek, 2013). Glutamate was absorbed upon diffusing 500 nm below the basal contact surface.

Estimating the number of vesicles released per ribbon to produce a threshold response in a cb2 cell

We calculated the number of vesicles released per ribbon to produce a threshold response in a cb2 bipolar cell as follows: The dynamic range for cb2 cell light response transients at low frequencies is on average 30.7 mV (Figure 1A). Using the relationship between cone capacitance change and cb2 EPSC amplitude figure Figure 5D, we infer that the midpoint of this range, 15.35 mV, corresponds to 2.3 vesicles released per ribbon ($\Delta C_{m(1/2)}$ = 2.3 fF, 0.05 fF/vesicle, and 20 ribbons per cone). We assign a threshold for transmitter release of 2 – 3 mV at the bipolar cell terminal, which, by linear extrapolation, corresponds to the release of roughly 0.3 – 0.45 vesicles per ribbon in the cones presynaptic to the recorded cb2 cell.

Estimating the number of glutamate molecules in a cone vesicle

The precise number of glutamate molecules in a cone vesicle is difficult to determine. We approached the problem by estimating the number of channels at a cb2 cell cone contact that are opened during the peak real mEPSC response and compared that to the number of channels that are opened by different vesicular glutamate concentrations in simulations. The maximal cb2 EPSC amplitude in our dataset was 378.5 ± 257.8 pA (n = 60 cells). The mean number of cb2 contacts per cone was 8.28 ± 4.76 (n = 4 cb2 cells and 41 contacted cones), so that the maximal EPSC amplitude per contact was 45.7 pA. Assuming a single-channel conductance of 12 pS (Ashby et al., 2008) and a reversal potential for bipolar cell cation channels of 0 mV, while noting that bipolar cells in these experiments were voltage-clamped at – 70 mV, we calculate that the single channel current is 70 mV x 12 pS = 0.84 pA. Thus 45.7/0.84 = 54.4 channels open on a single contact during a saturating glutamate pulse. Since we maximum open probability for the channel is ~70% (DeVries et al., 2006), we calculate that ~78 channels are expressed per dendritic tip. The mean cb2 mEPSC amplitude is 9.9 pA (DeVries et al., 2006), suggesting that the mEPSC opens almost a fourth of the maximum possible number of channels. In our simulations, this amplitude corresponds to 4000 glutamate molecules per vesicle, which is a reasonable value based on the range of values encountered in the literature (Barbour and Hausser, 1997; Budisantoso et al., 2013; Clements, 1996; DiGregorio et al., 2007; Jonas et al., 1993; Nielsen et al., 2004; Rao-Mirotznik et al., 1998; Riveros et al., 1986; Savtchenko et al., 2013). This is the concentration of glutamate that we chose. Other efforts, based on measurements of vesicular glutamate concentration and vesicle diameter, have led to two-fold lower estimates of glutamate concentration at the rod ribbon (Rao-Mirotznik et al., 1998). Matching our data to these estimates would require revision of our synapse geometry, our kinetic model, or our estimate for AMPAR single channel conductance.

Supplemental References

Ashby, M.C., Daw, M.I., and Isaac, J.T.R. (2008). AMPA Receptors. In The Glutamate Receptors, R.W. Gereau, and G.T. Swanson, eds. (Humana Press), pp. 1-44.

Barbour, B., and Hausser, M. (1997). Intersynaptic diffusion of neurotransmitter. Trends Neurosci 20, 377-384.

Budisantoso, T., Harada, H., Kamasawa, N., Fukazawa, Y., Shigemoto, R., and Matsui, K. (2013). Evaluation of glutamate concentration transient in the synaptic cleft of the rat calyx of Held. J Physiol 591, 219-239.

Clements, J.D. (1996). Transmitter timecourse in the synaptic cleft: its role in central synaptic function. Trends Neurosci 19, 163-171.

DiGregorio, D.A., Rothman, J.S., Nielsen, T.A., and Silver, R.A. (2007). Desensitization properties of AMPA receptors at the cerebellar mossy fiber granule cell synapse. J Neurosci 27, 8344-8357.

Herr, S., Ngo, I.T., Huang, T.M., Klug, K., Sterling, P., and Schein, S. (2011). Cone synapses in macaque fovea: II. Dendrites of OFF midget bipolar cells exhibit Inner Densities similar to their Outer synaptic Densities in basal contacts with cone terminals. Vis Neurosci 28, 17-28.

Jonas, P., Major, G., and Sakmann, B. (1993). Quantal components of unitary EPSCs at the mossy fibre synapse on CA3 pyramidal cells of rat hippocampus. J Physiol 472, 615-663.

Rao-Mirotznik, R., Buchsbaum, G., and Sterling, P. (1998). Transmitter concentration at a three-dimensional synapse. J Neurophysiol 80, 3163-3172.

Riveros, N., Fiedler, J., Lagos, N., Munoz, C., and Orrego, F. (1986). Glutamate in rat brain cortex synaptic vesicles: influence of the vesicle isolation procedure. Brain Res 386, 405-408.

Savtchenko, L.P., Sylantyev, S., and Rusakov, D.A. (2013). Central synapses release a resource-efficient amount of glutamate. Nat Neurosci 16, 10-12.

Schein, S., Ngo, I.T., Huang, T.M., Klug, K., Sterling, P., and Herr, S. (2011). Cone synapses in macaque fovea: I. Two types of non-S cones are distinguished by numbers of contacts with OFF midget bipolar cells. Vis Neurosci 28, 3-16.

Sobolevsky, A.I., Rosconi, M.P., and Gouaux, E. (2009). X-ray structure, symmetry and mechanism of an AMPA-subtype glutamate receptor. Nature 462, 745-756.

Stiles, J.R., Van Helden, D., Bartol, T.M., Jr., Salpeter, E.E., and Salpeter, M.M. (1996). Miniature endplate current rise times less than 100 microseconds from improved dual recordings can be modeled with passive acetylcholine diffusion from a synaptic vesicle. Proc Natl Acad Sci U S A 93, 5747-5752.